Hybrid Mechanistic–Empirical and 3D FEM Analysis of Airport Pavement under Heavy Aircraft Loads

Tukimun
Department of Civil Engineering, 17 Agustus 1945 University, Samarinda, Indonesia
moonix.mgt@gmail.com (corresponding author)

Miswar Tumpu
Disaster Management Study Program, The Graduate School, Hasanuddin University, Indonesia
tumpumiswar@gmail.com

Aco Wahyu Efendi
Department of Civil Engineering, Sebelas Maret University, Surakarta, Indonesia
acowahyudiefendi@student.uns.ac.id

Hoong-Pin Lee
Department of Civil Engineering, Faculty of Engineering and Quantity Surveying, INTI International University, Malaysia
hoongpin.lee@newinti.edu.my

Andung Yunianta
Department of Civil Engineering, Yapis University, Jayapura, Indonesia
andung.ay@gmail.com

Received: 8 March 2026 | Revised: 9 April 2026 | Accepted: 17 April 2026

 DOI: https://doi.org/10.48084/etasr.18604

ABSTRACT

This study evaluates airport pavement performance under heavy multi-wheel aircraft using a hybrid Mechanistic–Empirical (M–E) and 3D Finite Element (FE) approach. The framework combines Federal Aviation Administration Rigid and Flexible Iterative Elastic Layered Design (FAARFIELD) with detailed 3D FE modeling to assess stress, strain, fatigue, and rutting. A flexible runway and rigid concrete apron were analyzed under wide-body aircraft at maximum landing weight. M–E results indicated a fatigue damage factor of 0.60 and a rutting of about 5 mm over a 50-year period, showing rutting as the main distress for flexible pavement. FE simulations captured localized stress beneath wheels and predicted an instantaneous vertical displacement of 3.55 mm, consistent with mechanistic results. The agreement between the two methods confirms structural adequacy while highlighting proximity to rutting limits. This hybrid approach improves long-term performance predictions and supports resilient, sustainable airport infrastructure aligned with Sustainable Development Goals.

Keywords-mechanistic–empirical design; finite element analysis; airport pavement; heavy aircraft loading; fatigue life; rutting performance; structural response; resilient infrastructure; SDGs

I. INTRODUCTION

Airport pavements face severe loading due to wide-body aircraft, higher tire pressures, and complex multi-wheel landing gear. Unlike highways, airport pavements must withstand concentrated loads of several hundred kilonewtons per wheel during landing and taxiing. Structural response in layered pavements is governed by stress distribution, tensile strain, and subgrade deformation. Traditional empirical design methods are being replaced by Mechanistic–Empirical (M–E) frameworks, which combine stress–strain analysis with performance prediction to ensure reliability, optimize materials, and improve long-term serviceability [1, 2].

Federal Aviation Administration Rigid and Flexible Iterative Elastic Layered Design (FAARFIELD) implements the M–E approach and is widely used for airport pavement design. Its layered-elastic theory calculates critical tensile strain at asphalt layer bottoms and compressive strain at the subgrade top to predict fatigue cracking and rutting, respectively [3]. Studies have validated the effectiveness of M–E in predicting flexible pavement fatigue life and permanent deformation [4, 5]. However, layered-elastic solutions assume axisymmetric loads, homogeneous layers, and simplified boundaries, limiting their ability to capture localized stress concentrations, especially near slab edges, joints, and multi-wheel gear interactions [6].

Three-dimensional Finite Element (FE) modeling overcomes these limitations by representing tire–pavement contact areas, non-uniform stress fields, and complex inter-layer interactions [7, 8]. FE models quantify stress concentrations and bending in rigid slabs more accurately than Westergaard-based methods [9], while flexible pavement FE analyses reveal localized strain amplifications not captured by layered-elastic models [10]. Nonetheless, FE analysis alone does not provide long-term predictions of cumulative fatigue or rutting. Comparative studies indicate that layered-elastic models reasonably estimate global strains, but discrepancies occur near critical zones, with prior research rarely integrating long-term M–E life prediction with high-resolution 3D structural response analysis [11–13].

Heavy multi-wheel gear systems, such as Boeing 777 and Airbus A340, introduce complex stress superposition effects. Rutting often governs flexible pavement performance when subgrade strain approaches critical thresholds, even if fatigue criteria are satisfied [14-16]. Limited studies have evaluated how closely airport pavements operate near rutting limits using both M–E and 3D FE approaches. Ensuring resilience and sustainability in long-design-life pavements requires accurate structural response prediction, optimized material usage, and minimized lifecycle impacts. Existing studies address either numerical modeling accuracy or performance-based design, but comprehensive hybrid M–E and 3D FE frameworks remain insufficiently explored.

In this study, the hybrid M–E approach explicitly integrates long-term performance prediction from FAARFIELD with high-resolution 3D FE simulations. M–E predicts fatigue cracking and rutting progression via strain-based transfer functions and traffic spectra, while FE provides detailed stress, strain, and displacement fields under multi-wheel aircraft loading. The hybrid framework cross-compares global performance indicators, such as the Cumulative Damage Factor (CDF) and rutting depth, with localized mechanical responses to improve reliability and interpretation. This study aims to develop and demonstrate such a hybrid evaluation framework, assessing pavement adequacy, identifying governing distress mechanisms, and highlighting the added value of combining FAARFIELD and 3D FE modeling within a unified analytical approach.

II. METHODOLOGY

Slight differences in material modulus values between the FAARFIELD and the FE model arise from differences in modeling assumptions and calibration. FAARFIELD uses internally calibrated modulus values linked to its M–E transfer functions, while the FE model adopts representative elastic properties within standard material ranges. To ensure analytical consistency, the FE modulus values were kept within the same order of magnitude as those in FAARFIELD. A sensitivity analysis of ±20% was conducted to verify that structural responses do not rely on a single parameter set. Consequently, comparisons between the two approaches emphasize trends and relative agreement rather than exact numerical equivalence.

A. Pavement Structure and Materials

The current study evaluates flexible and rigid airport pavements designed for a 50-year service life at VVIP/VIP Nusantara International Airport (IKN) in Nusantara Capital City. The runway and fast taxiways consist of flexible asphalt pavement with a total thickness of ~103 cm, including dense-graded asphalt concrete (P401), stabilized base (P403), crushed aggregate base (P209), and granular subbase (P154), while the main apron uses a rigid pavement of ~116 cm with jointed plain concrete slab (P501) over a lean concrete base (P306), crushed aggregate base, and granular subbase (Figure 1). The subgrade assumes a minimum California Bearing Ratio (CBR) of 6%, corresponding to an elastic modulus of ~60 MPa via FAARFIELD (E=10×CBR), with minor acceptable variations. The material properties for stress–strain analysis are summarized in Table I. The thickness of each material was determined iteratively using FAARFIELD to meet fatigue and rutting criteria, and the heliport slab was excluded for consistency. Flexible pavements are evaluated based on strain-driven fatigue and rutting, while rigid pavements are assessed through flexural stress and repeated-load fatigue relationships, with mechanisms treated independently.

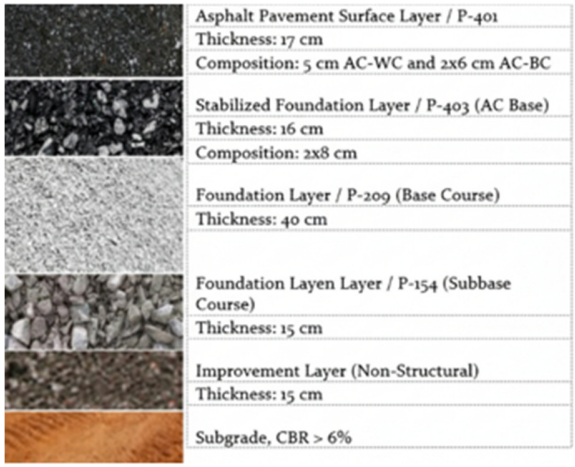

Fig. 1. Thickness of runway and taxiway pavement at VVIP/VIP IKN airport.

TABLE I. MECHANICAL PROPERTIES OF FLEXIBLE PAVEMENT LAYERS USED IN THE ANALYSIS

Layer Description	Thickness (cm)	Elastic modulus, E (MPa)	Poisson's ratio, ν	Unit weight, γ (kN/m³)
Asphalt surface course (AC-WC and AC-BC)	17	3500	0.35	23.0
Asphalt treated base (AC base)	16	2800	0.35	22.5
Base course (granular)	40	300	0.35	21.0
Subbase course (granular)	15	150	0.40	20.0
Improvement layer	15	100	0.40	19.5
Subgrade (CBR > 6%)	—	70	0.45	19.0

B. Model Assumptions

Both M–E and FE analyses were performed under consistent simplifying assumptions. Pavement layers were considered homogeneous, isotropic, and linear-elastic, without time-dependent viscoelastic behavior of asphalt or nonlinear plasticity of granular materials, to enable comparison of elastic structural responses between M–E and 3D FE approaches. Loading was treated as static for the critical gear configuration under maximum landing weight with a dynamic load amplification factor of 1.2, while thermal gradients and moisture-induced stiffness variations were neglected. Perfect bonding was assumed between layers, implying no interlayer slip, consistent with the FAARFIELD philosophy. For rigid pavements, interface conditions were simplified, without modeling dowel action or aggregate interlock, so the results are interpreted with this limitation in mind, ensuring consistent cross-comparison between layered-elastic and FE simulations.

C. Boundary Conditions

FE models employed boundary conditions to approximate an infinite pavement domain. The bottom boundary was fully fixed (zero vertical displacement) to represent a rigid support at depth, while lateral boundaries used roller constraints (zero normal displacement) to prevent rigid body motion; yet they allow tangential deformation. Axisymmetric models defined the central axis as a symmetry boundary, and 3D simulations incorporated symmetry planes where possible to reduce computational demand. Model dimensions extended laterally and vertically to several tire radii from the load zone to minimize boundary reflection effects. These boundary conditions follow established pavement FE modeling practices, ensuring that stress fields near wheel loads remain unaffected by artificial constraints.

D. Material Modeling

Material properties were assigned based on [17] and standard airport pavement specifications. Asphalt concrete layers were given $E \approx 3500$ MPa and $\nu \approx 0.35$, while the Cement-Treated Base (CTB) had $E \approx 800$ MPa, and granular base/subbase layers ranged between 150–300 MPa. The subgrade modulus was 60–70 MPa ($\nu = 0.35$) for consistency with FAARFIELD assumptions, with FE validation models using approximately 300 MPa to represent stiff soil (CBR>6%). For rigid pavement, Portland cement concrete slabs were assigned $E \approx 30{,}000$ MPa and $\nu \approx 0.20$. All materials were modeled as linear-elastic to enable direct comparison with FAARFIELD's layered-elastic framework, while nonlinear behavior was not considered to maintain analytical consistency.

E. Load Representation

Aircraft loading was represented using the most significant wide-body aircraft, namely the Boeing 777-300ER (Maximum Takeoff Weight = 352.4 t) and Airbus A340-500 (Maximum Takeoff Weight = 369.2 t), with main landing gear explicitly modeled (six-wheel bogies for B777, four-wheel bogies for A340). Each wheel load was applied as a uniform contact pressure over a circular tire imprint of ~0.7 m diameter, with conservative pressures of 1.2–1.6 MPa, amplified by a dynamic factor of 1.2 to account for landing effects. In FAARFIELD, equivalent single or multiple wheel loads were applied following FAA gear load conversion, with critical horizontal tensile strain at the bottom of asphalt layers and vertical compressive strain at the top of subgrade computed for flexible pavements, and slab flexural tensile stresses evaluated for rigid pavements. Rutting was interpreted from subgrade strain using strain-based transfer functions rather than direct empirical rut depth, while the tire contact diameter was based on typical wide-body aircraft dimensions per FAA guidance and literature.

F. Mesh Convergence Study

A mesh convergence study was conducted in LISA FEA v8 for both 2D axisymmetric and 3D models, with element sizes progressively refined near tire contact areas where stress gradients are the highest. Convergence was assessed by monitoring peak vertical stress beneath the wheel and maximum tensile stress at slab edges, while mesh density was increased until stress variations between successive refinements were below 5%. The final models used refined hexahedral elements for 3D and quadrilateral elements for 2D, with localized densification beneath each wheel footprint, ensuring that the reported stress and strain results are independent of the mesh discretization effects.

G. Validation Procedure

Validation was conducted by cross-comparing FAARFIELD mechanistic outputs with high-resolution FE results. For flexible pavement, bottom-of-asphalt tensile strain and top-of-subgrade compressive strain from FE simulations were compared with layered-elastic predictions, whereas for rigid pavement, slab-edge tensile stresses from FAARFIELD were assessed against maximum principal stresses from 3D FE models. Agreement in both magnitude and critical stress locations was evaluated. Fatigue CDF was computed using Miner's rule based on FAARFIELD traffic simulations, and rutting potential was assessed using subgrade strain criteria. Overall consistency between FE stress distributions and FAARFIELD predictions confirmed the structural adequacy of the pavement design.

H. Reproducibility

To ensure reproducibility, all input parameters, including layer thicknesses, elastic moduli, Poisson's ratios, wheel loads, contact pressures, and boundary conditions, are explicitly reported. The FAARFIELD version (2.0.7) and LISA FEA version (v8) are specified, and model geometry, mesh

refinement, and convergence criteria are described in detail to allow independent reconstruction. Traffic assumptions, aircraft configurations, and dynamic load factors are documented. By combining standardized FAA design procedures with transparent FE modeling parameters, this study provides a reproducible hybrid framework for evaluating airport pavement structural response under heavy aircraft loading.

III. RESULTS AND DISCUSSION

The results of the hybrid analysis, integrating M–E (FAARFIELD) predictions with three-dimensional FE simulations, demonstrate that FAARFIELD provides global performance indicators, such as fatigue life and rutting progression, whereas 3D FE captures localized stress concentrations, strain distributions, and displacements under multi-wheel aircraft loading. Emphasis is placed on the consistency between these approaches, as the hybrid framework's validity relies on FE results supporting or explaining mechanistic predictions. The discussion focuses on both overall performance outcomes and how FE simulations enhance the interpretation of mechanistic pavement behavior.

A. Stress and Strain Distribution under Aircraft Wheel Loads

The load application and stress propagation on the flexible runway pavement under heavy aircraft loading are depicted in Figure 2 for the Boeing 777-300 configuration. Vertical compressive stress at the surface under a single main wheel reaches approximately 1.2 MPa, corresponding to the tire contact pressure, and attenuates with depth through the asphalt and granular layers. This multilayer stress dissipation aligns with M–E design principles and previous 3D FE studies, where stress decreases rapidly in the upper layers before stabilizing in the subgrade [1, 3, 10]. Such stress attenuation patterns are key indicators of structural adequacy in airport pavements under high wheel loads, while the rutting threshold strain range of ≈1500–2000 με follows established M–E design criteria [2, 15].

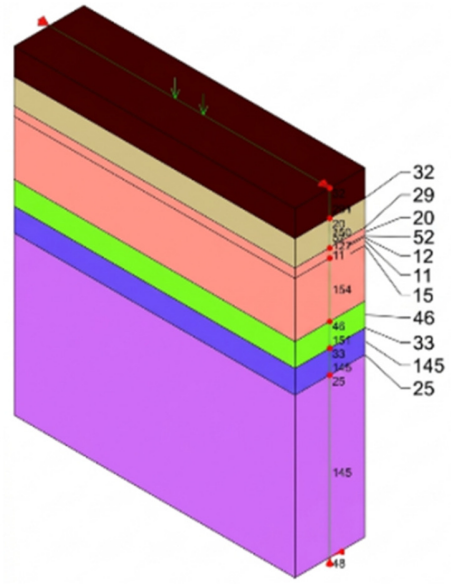

Fig. 2. Schematic of the gear loads on the runway cross-section.

At the bottom of the asphalt layer, horizontal tensile strain ranges between 150–250 με, below the fatigue threshold for dense-graded asphalt (~300–400 με), indicating adequate resistance to bottom-up fatigue cracking over a 50-year design life [2, 14], while vertical compressive strain at the top of the subgrade reaches 1200–1500 με, approaching typical rutting limits (~1500–2000 με) and suggesting that rutting governs long-term performance [2, 9, 15, 18]. FAARFIELD simulations show rutting damage factors slightly exceeding unity, consistent with nonlinear M–E analyses highlighting subgrade sensitivity to modulus reduction and moisture. The Boeing 777 rear-wheel footprint (~0.157 m²) supports ~174.83 kN per wheel, producing an average pressure of ≈1113.57 kN/m², matching FE stress magnitudes and illustrating localized stress amplification [7, 8]. Figure 3 presents von Mises stress distribution from LISA FEA, with maximum 1927 kN/m² beneath the tire and rapid attenuation with depth, confirming that critical responses are confined to upper layers [5, 10, 11] and emphasizing the importance of capturing localized peaks for accurate performance prediction [12]. Overall, pavement behavior is stiffness-controlled, with high stress observed in the upper layers but long-term deformation dominated by subgrade strain, consistent with recent mechanistic and AI-enhanced modeling studies [1, 3, 13, 14].

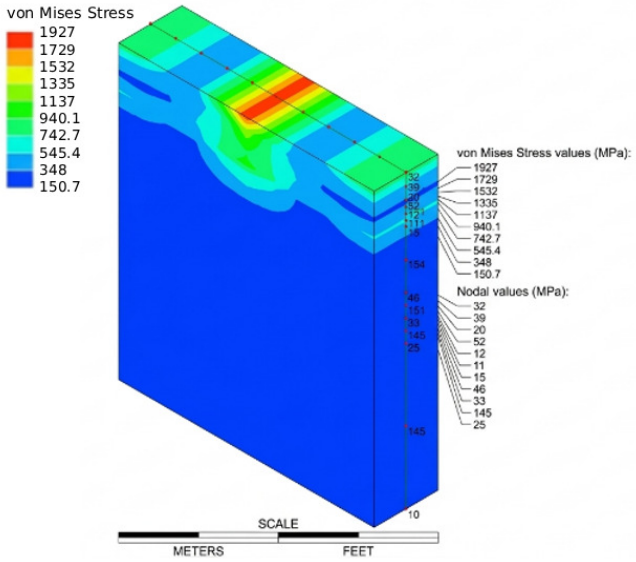

Fig. 3. Distribution of von Mises stress using LISA FEA.

B. Structural Response of Rigid Apron Pavement

The rigid apron pavement exhibits a distinct load-transfer mechanism through its 46 cm concrete slab, distributing wheel loads broadly before reaching the base and subgrade [1, 3]. Using the Westergaard slab theory, the maximum bottom-of-slab tensile stress under a ~700 kN main wheel load is ~0.4–0.5 MPa, providing a safety factor >8 against flexural cracking even with 20–30% dynamic amplification [4, 5, 11], while von Mises stress contours in Figure 3 show peaks near slab edges and beneath wheel loads, consistent with the slab-on-elastic-foundation behavior [6, 12]. FE validation and fatigue models confirm that tensile stress ratios well below unity correspond to

negligible fatigue over 50 years [4, 5, 11, 12], with edge deflections and temperature-induced curling limited by concrete stiffness under IKN's moderate thermal range (15–40°C) [3, 5, 11]. Unlike flexible pavements, performance is governed primarily by flexural stress relative to concrete strength rather than subgrade strain or cumulative deformation [2, 3], reinforcing that flexible pavements are strain-controlled through multilayer dissipation, whereas rigid slabs are strength-controlled, with performance dictated by tensile stress-to-strength ratios [1, 3]. The substantial safety margins confirm that the rigid apron ensures high structural reliability for heavy aircraft operations, and principal tensile stress is more appropriate than von Mises stress for brittle concrete failure assessment.

C. Fatigue Life Evaluation

The fatigue performance predicted by FAARFIELD is summarized using CDF analysis. For the flexible runway pavement, assuming approximately 100 annual heavy aircraft departures (B777/A340), the 50-year CDF is about 0.6, indicating that only 60% of the allowable fatigue life is consumed, with bottom-of-asphalt tensile strain remaining within acceptable mechanistic limits [1, 3]. Fatigue in flexible pavements is primarily governed by horizontal tensile strain at the asphalt bottom and vertical compressive strain at the subgrade, with predictions sensitive to strain-based transfer models and traffic spectra [2, 3]. AI and soft-computing studies show that tensile strains below critical thresholds minimize early cracking probability [13, 14]. For the rigid apron, the 46 cm slab yields a CDF below 0.1, with tensile stresses far below concrete flexural strength, confirming negligible fatigue accumulation over the design life [1, 3, 4, 5, 11]. This contrast highlights the significant difference in damage mechanisms: strain-controlled fatigue for flexible pavements versus strength-controlled performance for rigid slabs, reinforcing mechanistic principles and confirming that the proposed VVIP IKN Airport pavement configurations meet safe fatigue performance limits under projected traffic.

D. Rutting and Permanent Deformation

Permanent deformation (rutting) was evaluated using vertical compressive strain at the top of the subgrade and long-term FAARFIELD settlement predictions. Under the Boeing 777 loading scenario, cumulative rutting at the runway surface is approximately 5 mm over 50 years. Using subgrade strain as a rutting indicator aligns with M–E design frameworks, where permanent deformation is mainly governed by accumulated plastic strain under repeated loading [2, 3]. Research confirms that rutting progression in flexible pavements is highly sensitive to subgrade stiffness and traffic load magnitude, particularly for heavy aircraft operations [2].

The displacement magnitude distribution from LISA FEA is shown in Figure 4, with maximum instantaneous vertical displacement reaching approximately 0.00355 m (3.55 mm) at the wheel load center and gradually decreasing with depth, reflecting effective stiffness from the 22 cm CTB (P403) and granular layers [3, 10, 11, 15]. The FE model captures immediate elastic response, while FAARFIELD predicts cumulative deformation, with a displacement-to-settlement ratio of 0.71 (3.55 mm vs 5 mm), demonstrating strong agreement and confirming performance below the typical airport serviceability limit of 10 mm [1, 2, 3, 9, 12, 15]. The treated base enhances stiffness, reduces subgrade deformation, redistributes stress, and limits vertical strain transmission, lowering rutting damage factors [3, 15]. In contrast, the rigid apron transfers load primarily through flexural action, with deformation occurring at joints rather than subgrade shear, resulting in negligible permanent deformation and performance controlled by tensile stress-to-strength ratios rather than vertical compressive strain [2, 3].

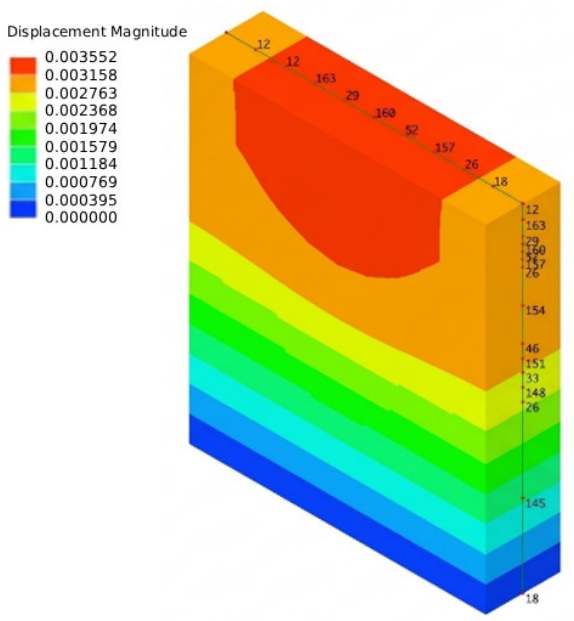

Fig. 4. Displacement magnitude distribution using LISA FEA.

E. Comparative Case: Airbus A340-500 vs Boeing 777-300ER

A comparative analysis between the Boeing 777-300ER and Airbus A340-500 shows that although the A340 has a slightly higher maximum take-off weight (369 t), its load distribution over more wheels reduces localized stress concentrations and improves load dispersion [6, 7, 8]. FE results indicate that peak strains under the A340 are comparable or slightly lower than those of the 777, with fatigue CDF being approximately 0.55 versus 0.60, and rutting strain levels near the threshold values [2, 3], confirming that fatigue and rutting responses are influenced by wheel load, tire pressure, and gear configuration in addition to aircraft weight. The 103 cm flexible pavement thickness provides adequate structural performance for both aircraft types, with Pavement Classification Rating PCR≥80 satisfying [17] for heavy international operations [1, 3]. Integrated FAARFIELD and 3D FE analysis shows that fatigue life is within acceptable limits, while rutting governs long-term performance, reflecting strain-controlled behavior [2, 15]. The rigid apron exhibits substantial structural redundancy with flexural stresses well below concrete capacity [3, 4]. The hybrid approach, combining M–E predictions and detailed 3D FE modeling, enhances design reliability by cross-validating empirical damage models with

mechanistic stress–strain responses [1, 3, 12], providing an understanding of governing distress mechanisms and supporting the structural adequacy of VVIP/VIP IKN Airport pavements under heavy aircraft loading.

F. Sensitivity Analysis: Effect of ±20% Modulus Variation

A parametric sensitivity analysis was conducted by varying the elastic modulus (E) of the asphalt layer, CTB, and subgrade by ±20% to evaluate design robustness and material uncertainty. A 20% reduction in asphalt modulus increased bottom-of-asphalt tensile strain by 18–22%, raising fatigue CDF from 0.60 to 0.78, while a 20% increase reduced strain and CDF to 0.48, indicating that asphalt stiffness primarily governs fatigue with a minor effect on subgrade strain (<5%). CTB modulus variations significantly influenced subgrade strain: a 20% decrease raised vertical compressive strain to nearly 1650 με, exceeding rutting thresholds, while a 20% increase reduced strain by 10–13%, highlighting the CTB's role in load distribution and long-term deformation control [2, 3, 15]. Subgrade stiffness strongly affected rutting susceptibility, with a 20% reduction increasing compressive strain to ~1800 με and a 20% increase lowering long-term settlement to 4.2 mm, confirming its dominant influence on rutting, while comparative sensitivity ranking showed that asphalt modulus governs fatigue, subgrade modulus governs rutting, and CTB acts as a balancing layer [1, 2, 3, 15]. Overall, the 103 cm flexible pavement is marginally optimized, meeting fatigue criteria (CDF≈0.6) but remaining sensitive to rutting under stiffness reduction; asphalt stiffening may improve fatigue resistance but risk brittleness, whereas subgrade softening accelerates rutting, emphasizing the importance of maintaining CTB stiffness. In contrast, the rigid apron shows minimal sensitivity to subgrade modulus, as performance is controlled by slab flexural rigidity, and vertical stress distribution under Boeing 777 loading (Figure 5) demonstrates nonlinear decay from surface to subgrade, consistent with the M–E theory [1, 3].

At the surface (depth=0 m), vertical stress reaches approximately 1.2 MPa, corresponding to tire contact pressure, and attenuates rapidly through the asphalt and treated base layers (0–0.33 m), while by the granular base (≈0.73 m depth) it drops below 0.2 MPa, confirming effective load spreading and structural dissipation (Figure 5). The steep stress gradient in the upper 30–40 cm indicates that the asphalt and stabilized base layers control peak stresses, whereas deeper subgrade stresses, though lower, produce high strain due to its reduced modulus, making deformation modulus-controlled rather than stress-controlled. Figure 6 exhibits vertical compressive strain increasing with depth under Boeing 777 loading, from ≈200–350 με near the stiff asphalt surface (E≈3500 MPa) to 1300–1450 με at 0.9–1.0 m depth at the subgrade, with the CTB mitigating strain amplification. This confirms that rutting governs flexible pavement performance despite decreasing stress, supports FAARFIELD's predicted ~5 mm long-term settlement, and validates M–E rutting assessment. From a design perspective, improving subgrade stiffness or base stabilization provides greater performance benefits than increasing asphalt thickness, highlighting the important role of foundation quality in heavy-aircraft airport pavements [1, 2, 3, 15].

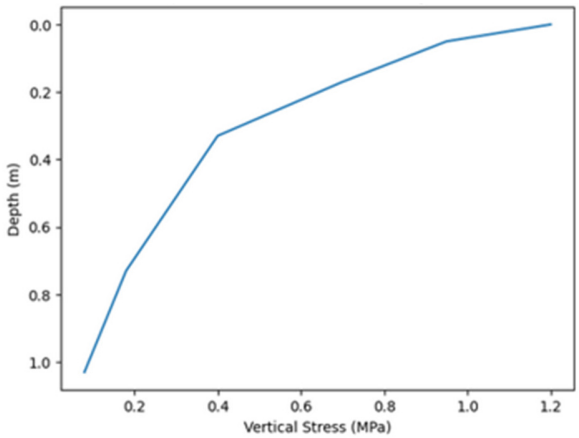

Fig. 5. Stress vs depth distribution under Boeing 777-wheel load.

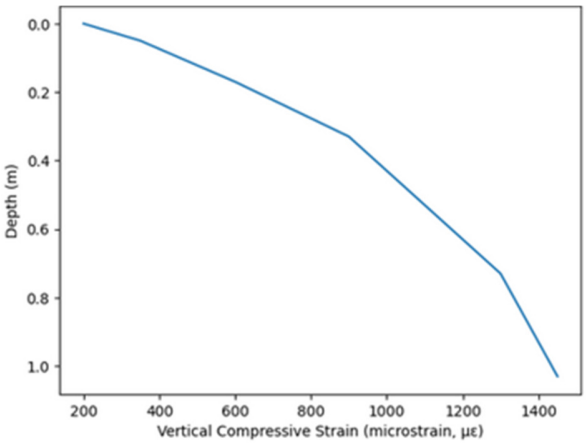

Fig. 6. Strain vs depth distribution under Boeing 777-wheel load.

G. Practical Engineering Implications and Future Research

The hybrid M–E and 3D FE evaluation provides practical insights for airport pavement engineering, showing that rutting driven by subgrade compressive strain, rather than fatigue cracking, governs flexible runway performance under heavy Boeing 777 and Airbus A340 loading. Sensitivity analysis indicates that a ±20% reduction in subgrade or CTB modulus can exceed allowable rutting limits, emphasizing the importance of construction quality, moisture control, and drainage, while rigid apron slabs offer higher structural redundancy under heavy static loads. The integrated FAARFIELD–3D FE framework enhances design confidence by combining long-term life prediction with localized stress-field validation, and stress–depth and strain–depth profiles confirm that structural performance is modulus-controlled, highlighting the benefits of foundation improvement (e.g., lime stabilization, geosynthetics, higher CBR) over marginal asphalt thickness increases [1, 2, 3, 15]. Future research should incorporate nonlinear constitutive models for granular and asphalt materials, advanced transient dynamic FE simulations, probabilistic reliability analysis, field validation with instrumented pavement sections, and sustainability assessment linking structural performance to lifecycle carbon footprint, while extending applicability to ultra-heavy and next-generation wide-body aircraft. This integrated approach cross-

validates cumulative damage with localized stress response, confirms rutting as the governing distress mechanism, and provides both theoretical understanding and actionable guidance for resilient airport pavement design [1, 2, 3, 15].

IV. CONCLUSION

This study developed a hybrid Mechanistic–Empirical (M–E) and 3D Finite Element (FE) framework to evaluate airport pavement structural response under heavy aircraft loading, integrating FAARFIELD-based performance prediction with detailed FE stress–strain analysis for consistent global and localized assessment. The 103 cm flexible runway satisfies fatigue requirements with a Cumulative Damage Factor (CDF) of approximately 0.6, while bottom-of-asphalt tensile strains remain within mechanistic limits, but vertical compressive strain at the subgrade approaches rutting thresholds, confirming permanent deformation as the governing distress mode. Sensitivity analysis (±20% modulus variation) shows that rutting is highly sensitive to reductions in subgrade and Cement-Treated Base (CTB) stiffness, highlighting the importance of foundation preservation and moisture control. Comparative analysis indicates that despite the Airbus A340-500's slightly higher weight, multi-wheel load distribution reduces localized strains, resulting in fatigue and rutting responses similar to or lower than the Boeing 777-300ER, validating the selected pavement thickness as a marginal but optimized design meeting Pavement Classification Rating (PCR) requirements. In contrast, the 46 cm rigid apron exhibits substantial structural redundancy, with flexural stresses being well below concrete capacity, fatigue CDF <0.1, and minimal sensitivity to subgrade variation, indicating strength-controlled performance rather than strain-driven distress. Overall, the hybrid approach confirms strong agreement between mechanistic strain evaluation and empirical life prediction, reinforcing confidence in structural adequacy, emphasizing rutting control for flexible pavements, and demonstrating that rigid pavements provide high reliability through strength-based resistance, supporting resilient, long-term airport infrastructure design.

DECLARATION OF COMPETING INTERESTS

The authors declare that they have no known financial interests, personal relationships, or affiliations that could have influenced the work reported in this paper.

ACKNOWLEDGMENT

The authors gratefully acknowledge the institutional support provided during the preparation of this study. Appreciation is extended to colleagues and technical staff who contributed to data processing and numerical modeling. The constructive insights from peer reviewers are also sincerely appreciated, as they have significantly improved the quality and clarity of this manuscript.

DATA AVAILABILITY

The data supporting the findings of this study can be made available from the corresponding author upon reasonable request. The data are not publicly available due to restrictions related to data ownership and institutional policies.

AI USE AND DECLARATION OF GENERATIVE AI USE

During the preparation of this work, the authors used generative AI tools to assist in language refinement and to improve the clarity of the manuscript. After using these tools, the authors carefully reviewed and edited the content as needed and take full responsibility for the final content of the publication.

REFERENCES

[1] J. Sun, E. Oh, G. Chai, Z. Ma, D. E. L. Ong, and P. Bell, "A systematic review of structural design methods and nondestructive tests for airport pavements," *Construction and Building Materials*, vol. 411, Jan. 2024, Art. no. 134543, https://doi.org/10.1016/j.conbuildmat.2023.134543.

[2] B. G. Famewo and M. Shokouhian, "A Review of Pavement Performance Deterioration Modeling: Influencing Factors and Techniques," *Symmetry*, vol. 17, no. 11, Nov. 2025, https://doi.org/10.3390/sym17111992.

[3] Y. Koh *et al.*, "Performance prediction models for flexible and rigid pavements – state-of-the-practice review for implementation in North America," *International Journal of Pavement Engineering*, vol. 26, no. 1, 2025, Art. no 2513454, https://doi.org/10.1080/10298436.2025.2513454.

[4] L. Bianchini Ciampoli, R. Pinto, and A. Benedetto, "Multivariate regression analysis for rapid fatigue prediction in airport rigid pavements," *Results in Engineering*, vol. 27, Sept. 2025, Art. no. 105959, https://doi.org/10.1016/j.rineng.2025.105959.

[5] K. K. Mathi and K. Nallasivam, "Dynamic and Fatigue Life Prediction Analysis of Airfield Runway Rigid Pavement Using Finite Element Method," *Computational Engineering and Physical Modeling*, vol. 5, no. 3, pp. 1–23, 2022, https://doi.org/10.22115/cepm.2022.347999.1215.

[6] A. Joshi, "Influence of moving load, structure, temperature gradient, and wheel configuration on load transfer efficiency," M.S. thesis, Department of Civil and Environmental Engineering, Henry M. Rowan College of Engineering, New Jersey, USA, 2013.

[7] Y. Xiong *et al.*, "Triaxial contact stress characterization for autonomous rail rapid transit pavements using coupled vehicle-pavement dynamic simulation," *International Journal of Solids and Structures*, vol. 327, Mar. 2026, Art. no. 113809, https://doi.org/10.1016/j.ijsolstr.2025.113809.

[8] H. Lang, W. D. Villamil, and I. L. Al-Qadi, "3D tire–pavement contact stresses: physics-informed prediction approach," *International Journal of Pavement Engineering*, vol. 27, no. 1, Feb. 2026, Art. no. 2621970, https://doi.org/10.1080/10298436.2026.2621970.

[9] D. Chen, L. Chen, W. Yu, G. Liu, and Z. Qian, "Investigation on the interaction between autonomous vehicles and pavement rutting considering driving safety," *International Journal of Pavement Engineering*, vol. 26, no. 1, July 2025, Art. no. 2538055, https://doi.org/10.1080/10298436.2025.2538055.

[10] A. Nega, D. Gedafa, and H. Nikraz, "Stress and Strain Characteristics in Flexible Pavement Using Three-Dimensional Nonlinear Finite Element Analysis," *International Journal of Pavement Research and Technology*, vol. 17, pp. 1498–1512, June 2024, https://doi.org/10.1007/s42947-024-00422-2.

[11] Q. Meng, K. Zhong, Y. Li, and M. Sun, "Comparative Study on Mechanical Response in Rigid Pavement Structures of Static and Dynamic Finite Element Models," *Aerospace*, vol. 11, no. 7, July 2024, Art. no. 596, https://doi.org/10.3390/aerospace11070596.

[12] S. Jamieson and G. White, "Validating a finite element model for rigid aircraft pavement load transfer against full scale testing," *International Journal of Pavement Engineering*, vol. 25, no. 1, June 2024, Art. no. 2363943, https://doi.org/10.1080/10298436.2024.2363943.

[13] S. Ramadan, H. Kassem, A. ElKordi, and R. Joumblat, "Incorporating Artificial Intelligence Applications in Flexible Pavements: A Comprehensive Overview," *International Journal of Pavement Research and Technology*, vol. 19, pp. 902–927, Apr. 2026, https://doi.org/10.1007/s42947-024-00496-y.

[14] G. Kaur and R. Kumar, "Assessing Fatigue and Rutting Life of Flexible Pavements Using Soft-Computing Techniques," *Journal of Failure Analysis and Prevention*, vol. 25, pp. 1256–1272, June 2025, https://doi.org/10.1007/s11668-025-02176-w.

[15] A. R. Ghanizadeh, M. Salehi, and F. Jalali, "Investigating the Effect of Lime Stabilization of Subgrade on the Fatigue & Rutting Lives of Flexible Pavements Using the Nonlinear Mechanistic-Empirical Analysis," *Geotechnical and Geological Engineering*, vol. 41, pp. 1287–1307, Mar. 2023, https://doi.org/10.1007/s10706-022-02336-x.

[16] S. E. Rasheed, M. Y. Fattah, W. H. Hassan, and M. Hafez, "Strength and Durability Characteristics of Sustainable Pavement Base Course Stabilized with Cement Bypass Dust and Spent Fluid Catalytic Cracking Catalyst," *Infrastructures*, vol. 9, no. 12, Nov. 2024, Art. no. 217, https://doi.org/10.3390/infrastructures9120217.

[17] *Airport Pavement Design and Evaluation*, AC 150/5320-6G, 2021

[18] Z. M. Aljaleel, N. Yasoub, and Y. K. H. Atemim, "Finite Element Modeling for Flexible Pavement Behavior under Repeated Axle Load," *Engineering, Technology & Applied Science Research*, vol. 14, no. 4, pp. 15180–15186, Aug. 2024, https://doi.org/10.48084/etasr.7505.